A HIGH-RESOLUTION QUICK-SCAN INTERFEROMETER FOR SOLAR STUDIES AT 3.75 GHz

Haruo TANAKA, Takakiyo KAKINUMA, Shinzo ÉNOMÉ,
Chikayoshi TORII, Yoshio TSUKIJI and Shoji KOBAYASHI

Abstract

A (32+2)-element compound interferometer for solar observations at 3.75 GHz has been in operation since August 1967. The HPBW is 23 seconds of arc for the compound and 1.1 minutes of arc for the 32-element adding interferometer. The outputs of these two kinds of interferometers are recorded at the same time with the sum and difference channels of two circularly polarized components. Artificial scanning of once each ten seconds by the adding interferometer has become possible since August 1968 for the observation of the rapidly changing burst.

1. Introduction

A compound interferometer composed of 32+2 dishes which is designed mainly for solar work at 3.75 GHz, has been completed at Toyokawa. It is the modernized enlargement of the 4-GHz interferometer constructed in 1953 (Tanaka et al. 1954, 1955) independently of the first Christiansen's interferometer. The new interferometer is quite similar to the east-west array of the 9.4-GHz interferometer (Kakinuma et al. 1963, Tanaka et al. 1965, 1967), and the two series of high-resolution scans are made at the same time.

Though the basic system is of conventional type aiming mainly at high resolution, there are three remarkable features. (1) The sum and the difference of two circularly polarized components are recorded in parallel. The observation of polarization becomes increasingly significant when the resolving power exceeds one minute of arc which is comparable with the source size (Tanaka et al. 1958). (2) Two series of scan curves are recorded at a time for two quantities mentioned above, the one being a scan curve taken with the 32-element adding interferometer and the other being a similar curve taken with the compound configuration. Four kinds of scan curves are recorded altogether. Since the compound interferometer always follows a certain ambiguity due to a severe need in tolerance, the simultaneous recording with the highly reliable adding

interferometer is quite desirable. It is to be mentioned that these two features are common with the 9.4-GHz interferometer. (3) For the 32-element adding interferometer, quick scanning at a speed of once each ten seconds is possible. Hence, the interferometric observations of the impulsive burst as well as the developing phase of the Type IV-μ have first become possible with almost sufficient time resolution.

The observations with a new interferometer started in August 1967 and the quick scanning device has been in operation since August 1968. Precise observations are now being made by taking a few drift curves around the central meridian passage of the sun and the rest of the time, two hours on both sides, is spent for quick scanning waiting for bursts. Some interesting results are already coming out from these observations (Énomé et al. 1969), and it is expected that the combination of 3.75-GHz and 9.4-GHz interferometers will furnish us with useful information available for the forecasting of proton flares (Tanaka et al. 1964), as well as for the study of active regions.

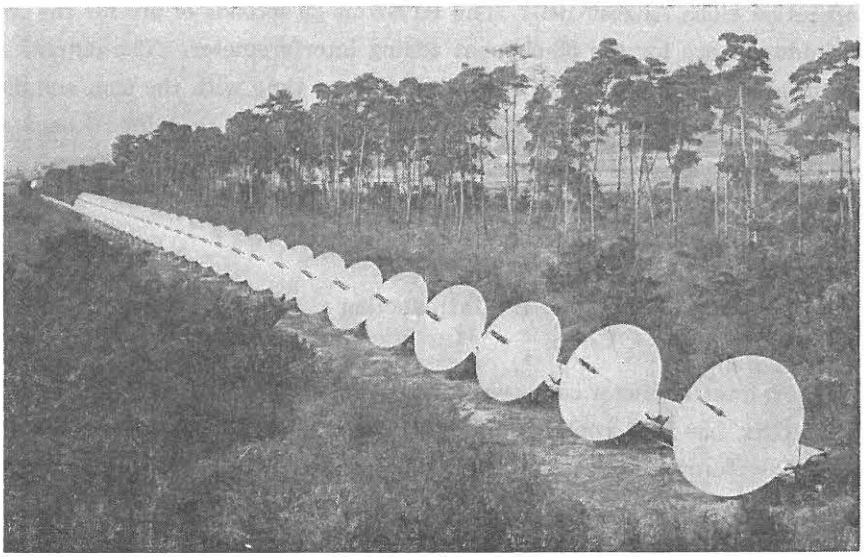

Fig. 1 General view of the 3.75-GHz compound interferometer.

2. Antenna System

The whole system of the interferometer is shown in Fig.2. Thirty-four 3-meter dishes are arrayed in a conventional form, each dish being on a polar mount. Thirty-three polar axes are driven by a common shaft and the remotest one is connected by synchros. Each declination axis is driven by a ratchet, which is fed by a programmed pulse train.

As is well known, the power pattern of the array is expressed as follows;

N-element adding array $$P_a(\theta)=\left[\frac{1}{N}\cdot\frac{\sin N\pi sx}{\sin\pi sx}\right]^2 \quad (1)$$

N+2 Compound array $$P_c(\theta)=\frac{1}{4N}\cdot\frac{\sin 4N\pi sx}{\sin\pi sx} \quad (2)$$

where,
$$\left.\begin{aligned} &s=d/\lambda \\ &x=\sin\theta \\ &\theta=\text{angle from the meridian plane}\end{aligned}\right\} \quad (3)$$

The main lobes exist at each θ where sx is equal to an integer and, since $s=86$ in our case, the lobe spacing is 40′ near the central meridian. The HPBW is 1.1′ for the adding interferometer and 23″ for the compound one.

The HPBW of a unit paraboloid is 2°, so that the sensitivity at the solar limb falls by a few percent when all the dishes follow the sun. Unfortunately, the step drive system (Tanaka et al. 1965) cannot be used as far as the artificial quick-scanning is made. The step drive system is adopted only for precise observations around the central meridian passage of the sun, when the drift scan is performed.

A simple branch system is used for combining the outputs of unit antennas, because it is the most economical and reliable system suitable for routine observations. A priority is put on high-resolution rather than sensitivity, since the solar work is the main objective and the reduced sensitivity due to the high-speed scanning is covered by an increased signal level during the burst.

3. Transmission Lines

As shown in Fig. 3, there is a quarter-wave plate and a ferrite switch just after the feed of each paraboloid for circular polarization measurement. The coil of the switch is fed by 60-Hz power line to get the enough magnetic field to operate a less sensitive ferrite of good temperature characteristic. The ferrite is so designed as to be saturated at $\pm\pi/4$ gyration of the electric vector so that quasi-rectangular modulation is performed. Following a couple of rotary joints of TM_{01} mode, the waveguide is guided under a long sun-shade. Alminium pipes, 83.63mm in inner diameter, are used for long transmission lines of TE_{11}-mode. The total transmission loss from the feeds to the input of the receiver is 3.8 db.

To avoid the mechanical stress due to temperature variation, flexible waveguides each 30 cm long are used. The waveguide is fixed on the ground at centers of the 32- and 2-element arrays as well as at the center of the whole base line. The length of the longest solid line is about 110 meters and its length changes by about 10 cm for the temperature change of 40°C. To avoid the phase variation, both ends of a flexible

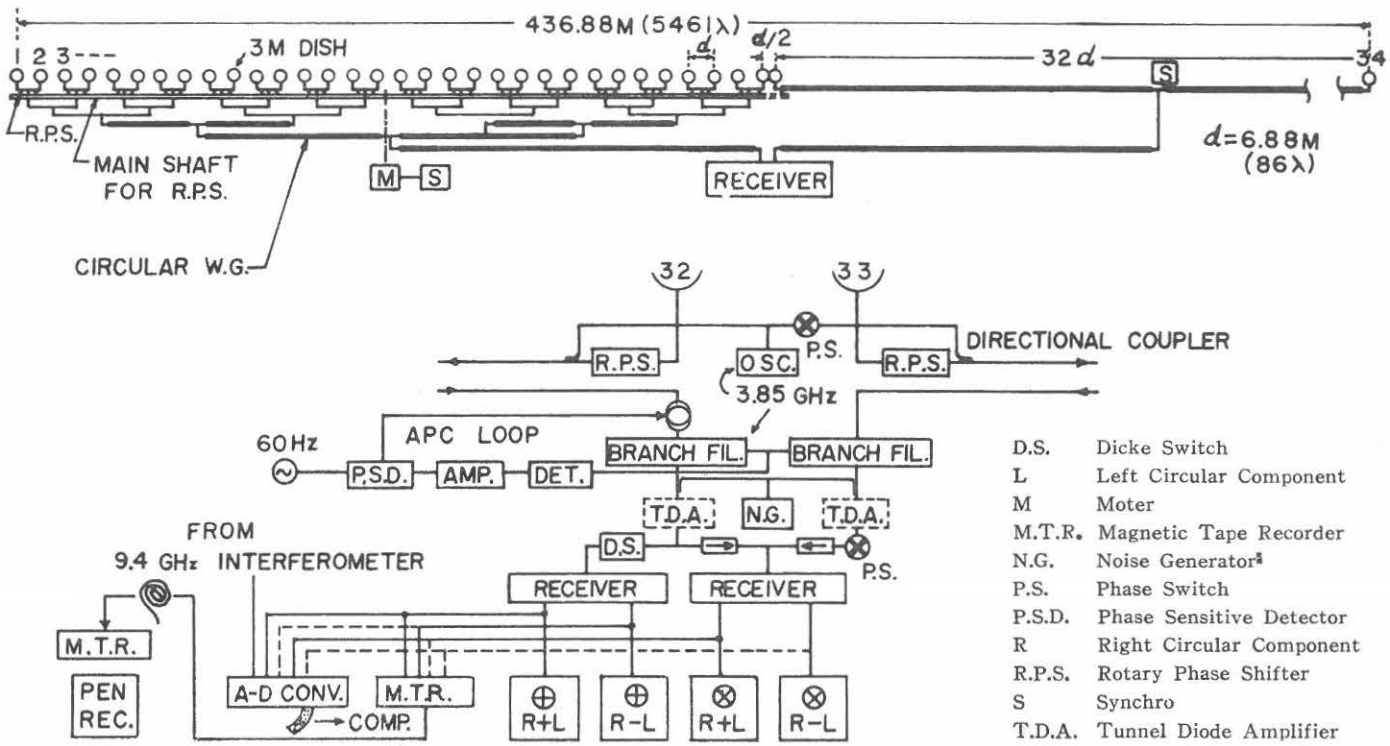

Fig. 2 The whole system of the 3.75 GHz compound interferometer

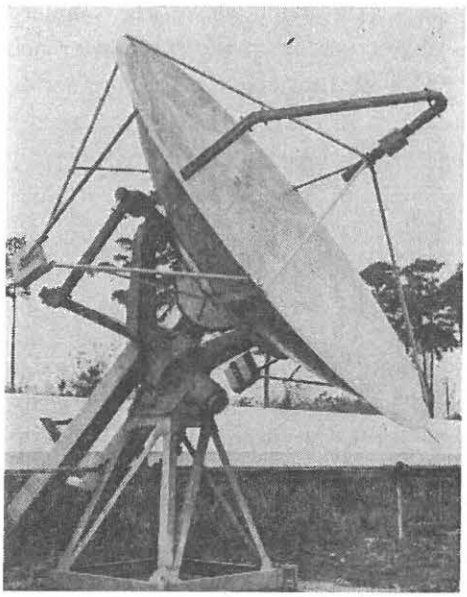

Fig. 3 Close-up view of element antenna

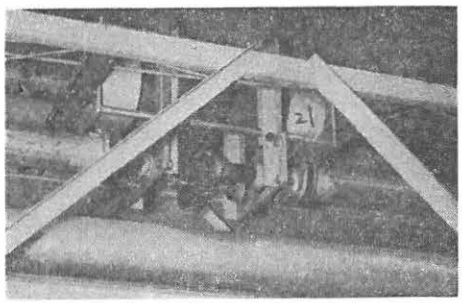

Fig. 4 A sample of rotary phase shifter

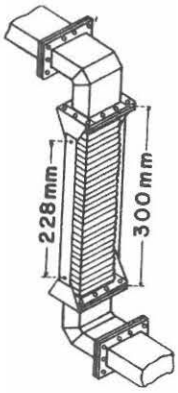

Fig. 5 Linked flexible waveguide

waveguide is linked as shown in Fig. 5. Let the length of flexible waveguide be L, and the displacement of the one end relative to the other be $\pm D$. Then the most suitable length of the link M can be calculated easily as,

$$M=3L/4+D^2/3L \tag{4}$$

For L=30 cm and D=5 cm, M=22.8 cm. It was verified by experiment that the phase change due to this device is less than 1 degree.

4. Automatic Phase Control

If the feeders are left unbound, the drift curve of the compound interferometer changes its shape considerably even during one scan, though the feeders are kept under the sun-shade and the path length is the same. We solved this problem by applying automatic phase control (APC) as shown in Fig. 2. The APC signal, 100 MHz apart from the receiving frequency, is divided into two, one of which being phase-modulated, and they are put into the output lines of No. 32 and 33 dishes. A fraction of the APC signal travels to the center of the 32- or 2-element interferometer and comes back to the receiver. They are combined again through branching filters, and a phase shifter

is controlled so as to nullify this combined signal. Since the amplitude of the combined signal is proportional to $\cos\phi$, ϕ being the phase corresponding to the path difference, the APC loop controls to make $\phi=\pi/2$. The phase of the signal channel must be adjusted once using a small active center on the sun. It has become clear that this partial APC system is enough to maintain a satisfactory performance.

5. Quick-Scanning Device

Following a proposal in 1965 (Tanaka, 1966), 32 rotary phase shifters are inserted in each output line of adding array as shown in Fig. 2. The rotary phase shifters are carefully adjusted, so that the maximum phase error during the rotation is less than 2°.

The phase shifters are driven continuously at different speeds as shown in Fig. 6. Sixteen kinds of gearing are coupled through a common shaft, whose speed is the same with that of the outermost phase shifters. The couplings of the shaft are quite flexible in axial direction, while it is quite rigid for a twist. The maximum twist angle of the shaft is less than 1.5 degrees, which corresponds to the maximum phase error of 3 degrees. One rotation of the slowest phase shifters corresponds to 4 scans, and the position mark is put on the record every time when the phase shifters pass through a standard position where they stop accurately when the off-switch is turned on.

When the lobes are swept at a frequency of f_s cycles per second, the directivity is expressed as:

$$P_a(\theta,t)=\left[\frac{1}{N}\cdot\frac{\sin N\pi sx-f_s(t-t_0)}{\sin\pi sx-f_s(t-t_0)}\right]^2 \tag{5}$$

where t_0 is the time when the phase shifters pass through a standard position. From the time of position marks and the time of a peak on the record, we can calculate without difficulty the position of the peak relative to the solar disk.

As this scanning system has been successfully realized, we are planning to extend it to the compound interferometer by adding two rotary phase shifters.

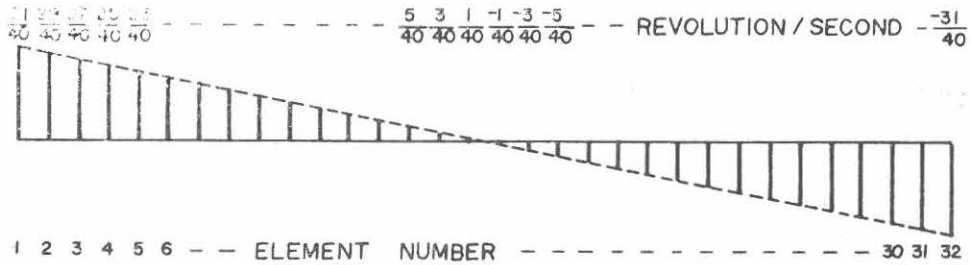

Fig. 6 Rotational speed of the rotary phase shifters.

6. Recording

Conventional drift curves are recorded on the pen recorders, an example of which is shown in Fig. 7. Digital recording is not yet completed but R+L channels including 9.4 GHz interferometer are now in routine operation. Fig. 8 shows an example of the output of the electronic computer, where the scale is calibrated with the flux density derived from radiometers. The sampling interval is just one eighth of the theoretical maximum value for the adding interferometer, and the interval is changed every day. The start of the A−D converter is controlled by a digital clock relay, whose dials are set according to the table.

A digital record of the compound channel is not only calibrated in the same manner, but also it is smoothed after the method of T.H. Legg (1964). They are drawn on the same sheet as shown in Fig. 9.

When the quick-scan is in operation, the record becomes as shown in Fig. 10. As the response time of the recorder is insufficient for the maximum possible frequency of 3 Hz, this record is available only as a real-time monitor. The available records are obtained later by reproducing the signal on the magnetic tape at a speed of one fourth that of recording. An example of the reproduced record is shown in Fig. 11.

Since the scanning speed is 16 times that of normal scan, the time constant must be reduced by the same amount. Hence, the fluctuation becomes four times as large as that of normal drift scan, but still the sensitivity seems to be enough for the observation of a burst.

7. Acknowledgement

The authors wish to express their sincere thanks to Messrs. T. Takayanagi and N. Yoshimi of Radio Astronomy Section, The Research Institute of Atmospherics for their valuable contribution to the construction of the equipment.

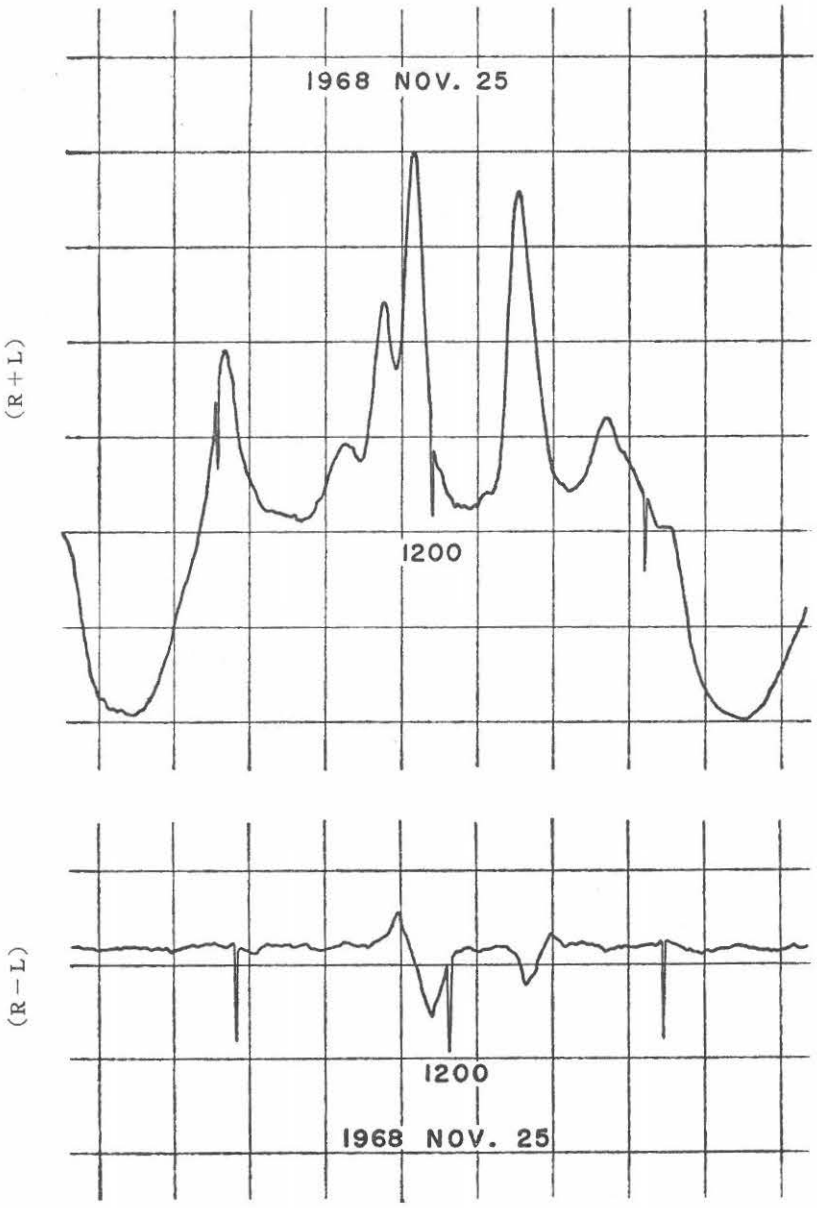

Fig. 7(a) Drift curves taken by the adding interferometer (HPBW 1′.1)

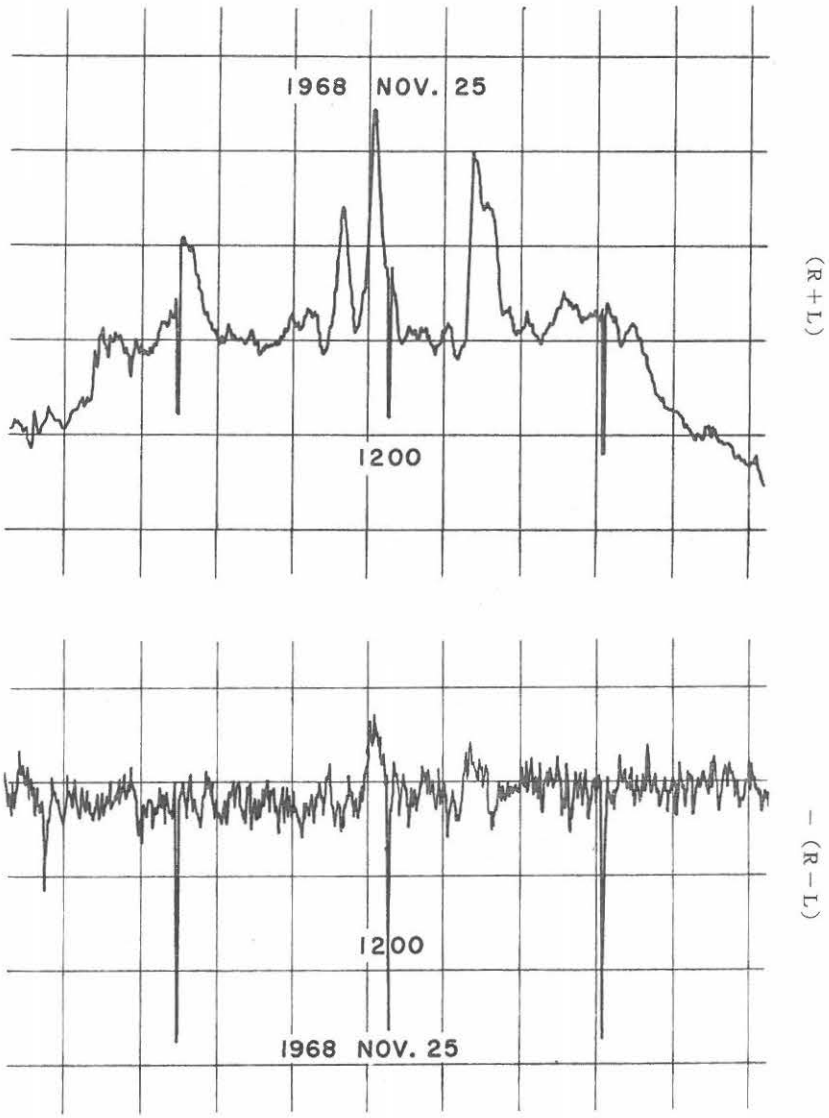

Fig. 7(b) Drift curves taken by the compound interferometer (HPBW 24″)

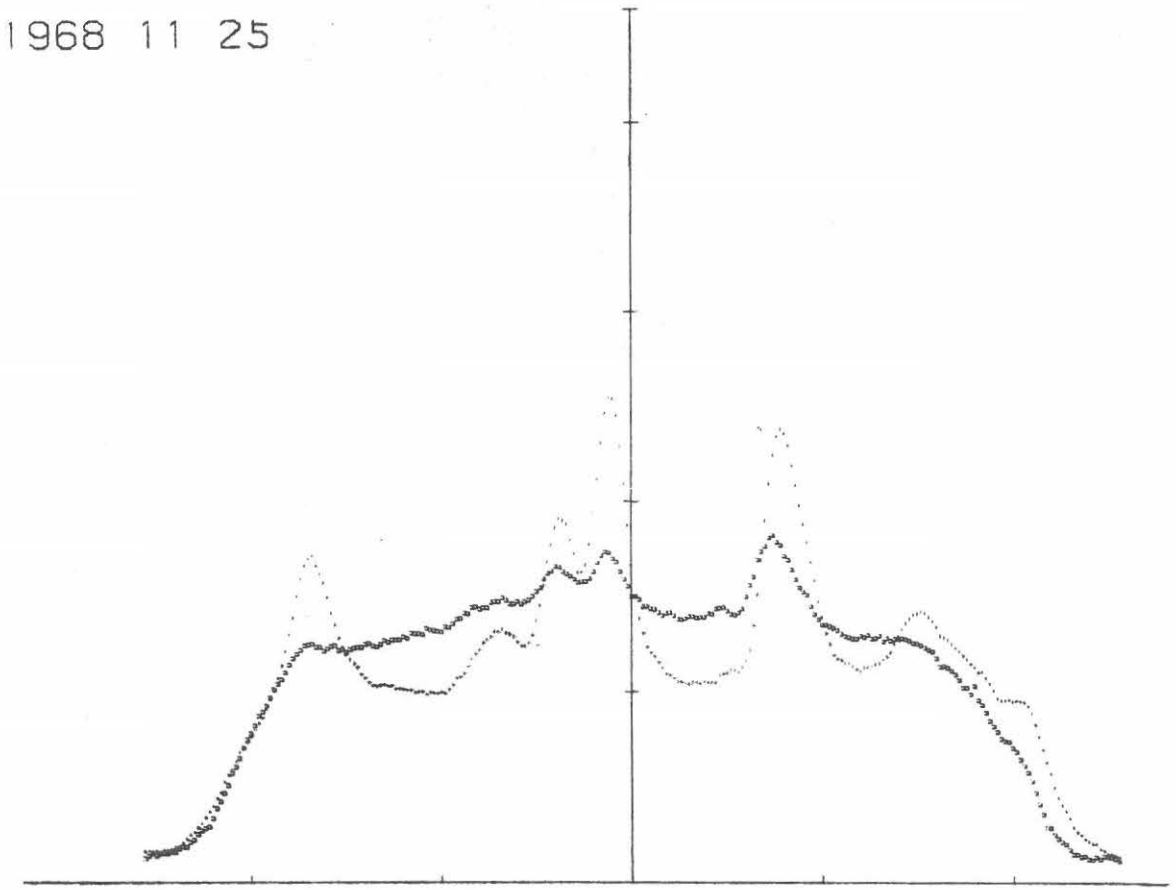

Fig. 8 Display of the drift curves corrected by electronic computer.
□:9.4 GHz and + :3.75 GHz. HPBW=1.1′.
(Flux/Area) for 9.4 GHz is twice the same ratio for 3.75 GHz.

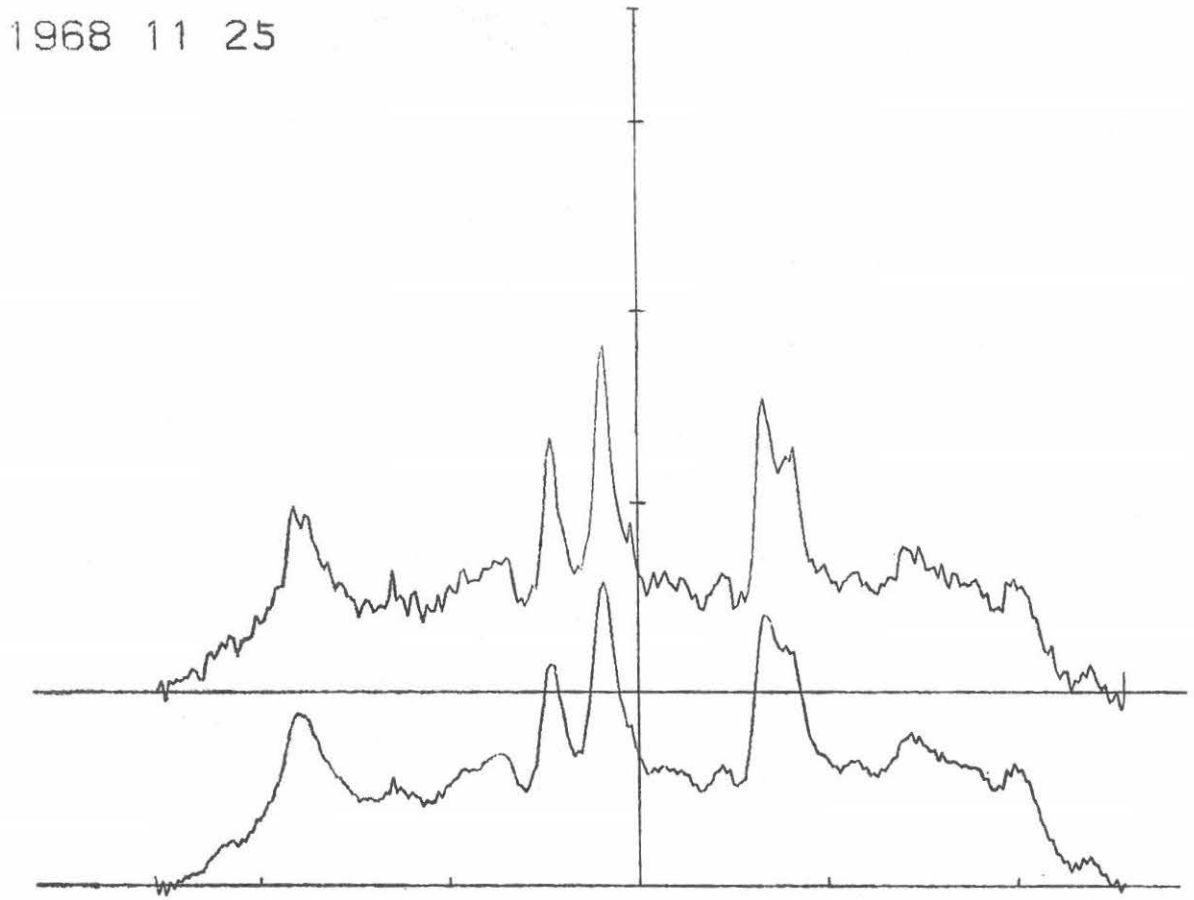

Fig. 9 Drift curves taken by the compound interferometer before and after smoothing: upper and lower respectively.

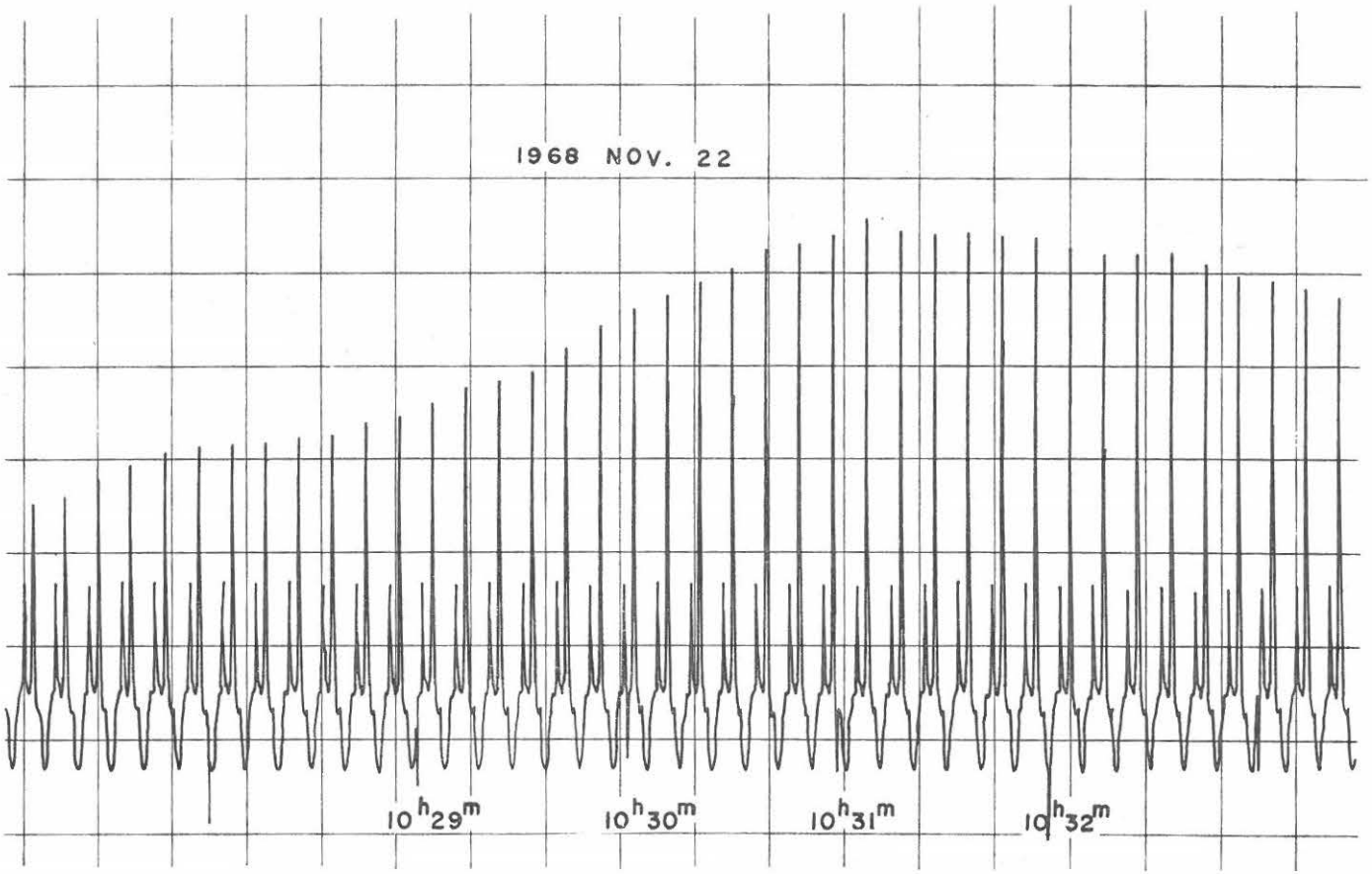

Fig. 10 Real time record of quick-scan used as a monitor.

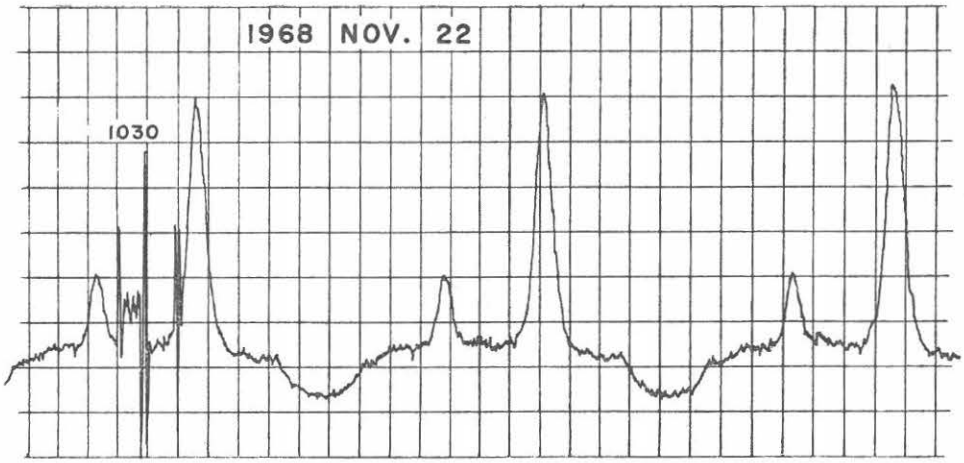

Fig. 11(a) Reproduced record of quick-scan.

(R + L)

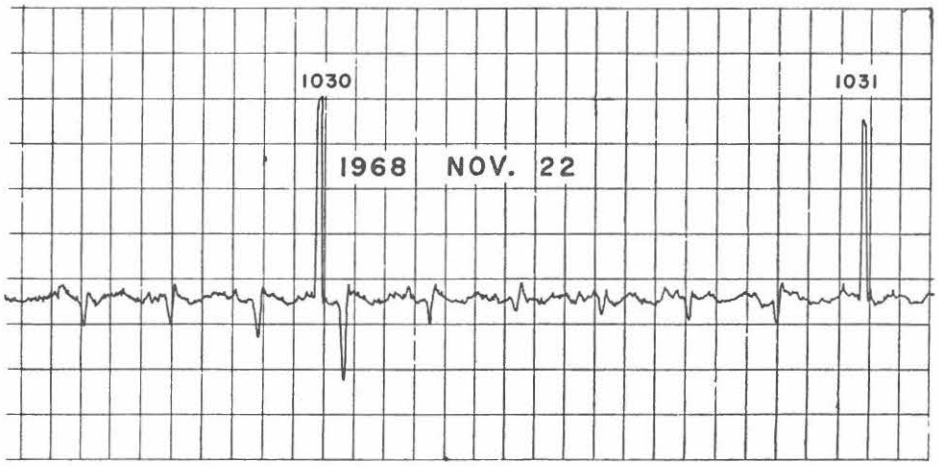

Fig. 11(b) Reproduced record of quick-scan.

(R − L)

References

Énomé, S., Kakinuma, T. and Tanaka, H. : High-Resolution Observations of the Solar Radio Burst with Multi-Element Compound Interferometers at 3.75 and 9.4 GHz, Solar Physics, **6**, 428 (1969)

Kakinuma, T. and Tanaka, H. : A High-Resolution Interferometer for Polarization Measurement at 9.4 Gc/s, Proc. Res. Inst. Atmospherics, Nagoya Univ., **10**, 25 (1963)

Legg, T. H. : Smoothing for Phase-Switched Radiotelescopes, Proc. P.I.E.E.E. Trans., **AP-12**, 6, 803 (1964)

Tanaka, H. and Kakinuma, T. : Multiple Element Interferometer for Locating Sources of Solar Noise at 4000 Megacycles, Proc. Res. Inst. Atmospherics, Nagoya Univ., **2**, 53 (1954), **3**, 102 (1955)

Tanaka, H. and Kakinuma, T. : Eclipse Observations of Microwave Radio Sources on the Solar Disk on 19 April 1958, Rep. Ionosph. Res. Japan, XII, 3 (1958)

Tanaka, H. and Kakinuma, T. : The Relation between the Spectrum of Slowly Varying Component of Solar Radio Emission and Solar Proton Event, Rep. Ionosph. Space Res. Japan, XVIII, 1, 32 (1964)

Tanaka, H. and Kakinuma, T. : Improvement of the High-Resolution Interferometer at 9.4 Gc/s, Proc. Res. Inst. Atmospherics, Nagoya Univ., **12**, 27 (1965)

Tanaka, H. : A Project of Multiple-Element Swept-Lobe Interferometer for the Study of Solar Radio Bursts, Proc. Res. Inst. Atmospherics, Nagoya Univ., **13**, 49 (1966)

Tanaka, H., Kakinuma, T. and Enome, S. : High-Resolution Observations of the Sources of Solar Radio Burst at 9.4 Gc/s, Proc. Res. Inst. Atmospherics, Nagoya Univ., **14**, 23 (1967)